Analyst

Accepted Manuscript

This article can be cited before page numbers have been issued, to do this please use: L. Jiang, Y. Yang, Y. Lin, Z. Chen, C. Xing, C. Lu, H. Yang and S. Zhang, *Analyst*, 2020, DOI: 10.1039/D0AN00275E.

ROYAL SOCIETY OF CHEMISTRY

rsc.li/analyst

View Article Online
DOI: 10.1039/D0AN00275E

ARTICLE

An electrochemical sensor based on enzyme-free recycling amplification for sensitive and specific detection of miRNAs from cancer cells

Received 00th January 20xx,
Accepted 00th January 20xx

DOI: 10.1039/x0xx00000x

Lili Jiang[a], Yuling Yang[a], Yuhong Lin[a], Ziyi Chen[a], Chao Xing[a], Chunhua Lu[a]*, Huanghao Yang[a] and Shusheng Zhang[b]*

MicroRNAs (miRNAs) are desirable targets for the diagnosis, prognosis and treatment of diverse human diseases. In this study, we developed a universal and enzyme-free signal amplification approach for the quick, sensitive and specific electrochemical detection of diverse miRNAs from tumor cells using catalyzed hairpin assembly (CHA) and the DNA three-way junction (DNA TWJ). The target miRNA, which was formed as an initiator through specific recognition, periodically triggered the assembly of two hairpins into a duplex via CHA. Subsequently, these duplexes induced the catalytic assembly of the DNA three-way junction and the release of methylene blue-labeled DNA strands S (S-MB). Thereafter, the S-MB was captured by the electrode through hybridization with the capture probe to generate a notable current response. The proposed biosensor could be switched in response to different miRNA targets by changing the specific sequence of H0. These findings point to the ability to distinguish the single base mismatch miRNAs and to analyze miRNAs extracted from cells. Therefore, the universal and enzyme-free signal amplified electrochemical method described herein can be potentially useful in diverse miRNAs-related clinical analysis and disease diagnosis.

Introduction

MicroRNAs (miRNAs) are a class of small, endogenous and non-protein coding RNA molecules with a typical length of 19–22 nucleotides[1]. They play vital regulatory roles in diverse physiological processes such as cellular proliferation, differentiation and apoptosis[2-5]. Recently, increasing evidence has indicated that the pathogenesis of various human diseases[6], including cancers, cardiovascular diseases and neurological diseases, associates with the abnormal expression of miRNAs in cells[7-9]. MiRNA expression profiles can provide new insights on potentially valuable biomarkers and targets for the diagnosis and clinical analysis of early tumours and related diseases[10-12]. In light of this, it is critical to engineer fast, efficient and sensitive analytical techniques for the ultrasensitive detection of low expression level of miRNAs.

Traditional approaches for miRNA assays such as quantitative reverse transcription-polymerase chain reaction (qRT-PCR)[13], northern blotting[14]and microarray[15] have been proposed. However, some shortcomings of these methods limit their wide applications in clinical analysis, such as low sensitivity, poor specificity, time-consuming and operational complexity. Recently, several miRNA analytic methods based on electrochemiluminescence[16,17], photoelectrochemistry[18,19], surface plasmon resonance[20], fluorescence[21], chemiluminescence[22], and electrochemistry[23-26] have been widely reported. Of these methods, electrochemical miRNA biosensor as a highly sensitive technology has gained particular attention with the advantage of their simplicity, portability and low-cost. Many powerful signal amplification strategies such as nuclease-assisted amplification[27,28] have been successfully applied to increase the detection sensitivity of the electrochemical miRNA biosensors. Due to the 1: N recognition ratio pattern between target and probe molecules and the robust signal amplification ability, nuclease-assisted amplification has further contributed to ultrasensitive electrochemical miRNA detection. However, most of these amplification strategies require the use of one or several types of enzymes, which complicates the experiments. Moreover, false-positives may occur during the amplification. Thus, engineering ultrasensitive electrochemical miRNA biosensors without the need of nuclease is urgently needed.

Recently, catalyzed hairpin assembly (CHA), a robust and enzyme-free amplification technique, has gained research momentum in the signal amplification and detection of nucleic acid targets owing to its excellent properties[29-32]. In a typical CHA reaction, due to the intramolecular hybridization of the hairpin structures, the two elaborately hairpin structures

[a] MOE Key Laboratory for Analytical Science of Food Safety and Biology, Fujian Provincial Key Laboratory of Analysis and Detection Technology for Food Safety, State Key Laboratory of Photocatalysis on Energy and Environment, College of Chemistry, Fuzhou University, Fuzhou 350108, P.R. China.
[b] Collaborative Innovation Centre of Tumour Marker Detection Technology, Equipment and Diagnosis-Therapy Integration in Universities of Shandong, College of Chemistry and Chemical Engineering, Linyi University, Linyi 276005, P.R. China
E-mail address: chunhualu@fzu.edu.cn , shushzhang@126.com; Tel.: +86-591-22866135
Electronic Supplementary Information (ESI) available: DNA sequences used in this study, comparison between our established biosensor and reported methods, the detail PAGE images (PDF). See DOI: 10.1039/x0xx00000x

View Article Online
DOI: 10.1039/D0AN00255E

cannot interact with each other. The addition of an initiator strand can yield a hundred-fold catalytic amplification, thereby assigning the CHA reaction enormous signal amplification capability and operational flexibility[33,34]. In addition to the DNA assisted amplification technique, many stale DNA nanostructures also offer new insights on bioanalysis. For instance, the DNA three-way junction (DNA TWJ) consists of three complementary oligonucleotide branches with high stability, and it has been extensively applied in the construction of dynamic DNA assemblies and architectures[35-37].Despite present electrochemical biosensors targeting nucleic acids with its excellent analytical performance, one limitation is that a specific nucleic acid probe can only be used for the detection of each miRNA, which make it impossible to detect multiple miRNAs using the same probes. To overcome this challenge, a feasible solution is to convert the detection of multiple miRNAs into a unified alternative for subsequent signal transduction and quantification with the sane probes.

Herein, we developed an enzyme-free and universal electrochemical biosensor for the ultrasensitive detection of diverse miRNAs from cancer cells, which combines the advantages of CHA with the DNA TWJ (Scheme 1). In our design, the loop sequence of H0 was designed as recognition module to recognize the miRNA, which could extend the assay's recognition range from only specific miRNA to diverse miRNAs by changing the loop sequence of H0 to achieve multiple miRNAs detection using the same probes. So, the target miRNA specifically recognized H0, and the formed T/H0 was designed to serve as the universal initiator for amplification in the CHA system, resulting in the formation of H1/H2 duplexes and the release of T/H0. The liberated T/H0 was recycled to facilitate the CHA reaction and to accelerate the formation of H1/H2. Subsequently, H1/H2 duplexes hybridized with the DNA strand L to form the DNA TWJ and release methylene blue (MB)-labeled DNA strands S (S-MB) from L/S-MB duplexes. Thereafter, the released S-MB bound onto the electrode by hybridizing with the capture probe (CP), and notably amplified electrochemical signals were produced for the sensitive detection of miRNA. Therefore, this strategy could provide a universal platform for the highly selective and sensitive detection of miRNA in nascent stages of cancer.

Experimental section

Construction of the biosensor

At first, the gold electrode (AuE) was immerged in a fresh piranha solution (3:1 by volume of 98% H_2SO_4 and 30% H_2O_2) for 30 min. After washing thoroughly with ultrapure water, the AuE was polished sequentially with 0.3 and 0.05 μm alumina slurries, followed by ultrasonically treating in ethanol and ultrapure water for a few minutes. Finally, the electrode was electrochemically cleaned through successive potential scans (between −0.35 to 1.6 V) in a fresh H_2SO_4 solution (0.5 M) and dried with nitrogen to obtain the pretreated electrode.

Prior to probe immobilization, hairpin probes (H0, H1 and H2) were heated to 95 °C for 5 min followed by fast cooling 4 °C. Then the probes were stored at 4 °C for further use. 5 μL of 10 μM the thiol-modified CP was mixed with 5 μL of 10 mM TCEP for 1h to reduce the disulfide bonds. The mixture solution was subsequently diluted to the CP concentration of 0.5 μM with Tris-HCl buffer (20 mM, 100 mM NaCl, 5 mM $MgCl_2$, 5 mM KCl, pH 7.4) before use. 5 μL of diluted mixture was dropped onto the above AuE surface and allowed to react overnight at room temperature to create the CP/AuE. Subsequently, the CP/AuE was further passivated with MCH (2 mM) for 1 h to block the nonspecific adsorption sites to obtain the MCH/CP/AuE.

Amplified detection of miRNA

In the miRNA assay, different concentrations of the target were mixed with H0 (50 nM), H1 (200 nM), H2 (200 nM) and the partial DNA duplex (L/S-MB) (200 nM) in Tris−HCl buffer and incubated at 37 °C for 120 min in a microcentrifuge tube. Subsequently, 5 μL of the above reaction solution was dropped on the MCH/CP/AuE sensing electrode for 3 h at room temperature. Then, the sensing AuE was thoroughly washed with ultrapure water and carefully dried under nitrogen atmosphere.

Results and discussion

Design principle of the sensor

The working principle of the proposed electrochemical biosensor for the detection of miRNA is illustrated in Scheme 1. The CHA and DNA TWJ-based biosensing system included three hairpin probes (H0, H1 and H2), a thiol-modified capture probe CP and a duplex of DNA strands L and MB-labeled DNA strands S (L/S-MB). The sensing interface was constructed by the immobilization of the CP onto AuE via Au-S interactions. H0 contained two functional groups, namely, the recognized target sequence locked in the loop, which could extend the assay's recognition range from only specific miRNA to diverse miRNAs by changing the loop sequence of H0, and the CHA initiation sequence locked in the stem. In principle, CHA with the same designs can be used for detection of any miRNA target by simply changing the loop sequence of H0. Although H1 and H2 were designed with complementary sequences, they interlocked by intramolecular hybridization. Initially, the complementary sequences of L/S-MB were designed with 3 nt longer than the counterpart of S and the capture probe (CP), thereby leading to a higher stability of L/S-MB and a lower background signal. In the absence of target, H0, H1, H2 and L/S co-existed in the system, and no free S-MB was generated to hybridize with CP. After the target inputting, target specifically recognized H0 to form T/H0 and exposed the stem-locking region containing the CHA initiation sequence to trigger the CHA of H1 and H2. The displaced T/H0 was recycled to facilitate continuous CHA in order to generate copious amounts of H1/H2 duplexes. More importantly, the formation of H1/H2 brought the two single-strand tails of H1 and H2 into close proximity. The close tails could initiate displacement between H1/H2 and L/S-MB due to the significantly increased stability between L and the tail sequences of H1/H2.

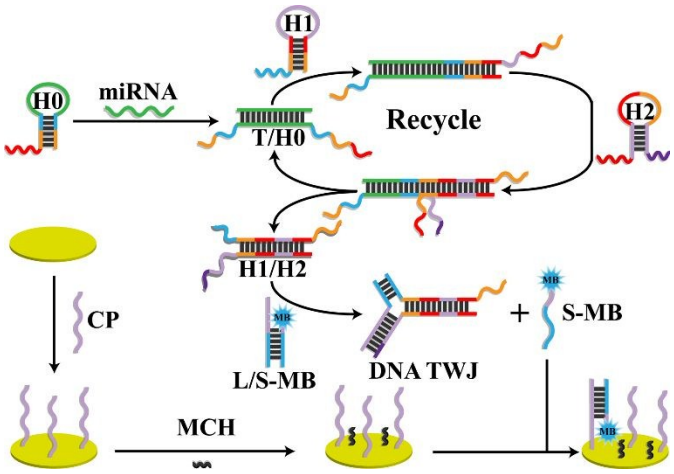

Scheme 1 Schematic diagram of the proposed biosensor for the miRNA assay.

Subsequently, the stable hybrid complex DNA TWJ was formed and S-MB was separated from L/S-MB. The released S-MB could then hybridize with the CP on the electrode, thereby leading to the highly sensitive detection of miRNA with a notably amplified signal.

Characterization of the biosensor

Electrochemical impedance spectroscopy (EIS) was first utilized to probe the electrochemical properties of the electrode interface during the stepwise assembly modification. $[Fe(CN)_6]^{3-/4-}$ redox probes were used to monitor and confirm the construction of the biosensor. As shown in Fig. 1A, the bare Au electrode displayed an extremely narrow semicircle (curve a), which reflected its excellent conductivity. After AuE was treated with CP, the charge transfer resistance (Rct) was enhanced (curve b) by the electrostatic repulsion between the negatively charged CP and $[Fe(CN)_6]^{3-/4-}$. Subsequently, the Rct was further increased by blocking the electrode surface with MCH (curve c). In the absence of target miRNA, the co-existence of H0, H1, H2 and L/S showed a negligible effect on the Rct (curve d). In the presence of target miRNA, the biosensor was activated, and S hybridized with CP on the electrode, thereby significantly increasing the Rct (curve e). The results of all experiments confirmed the successful development of the proposed electrochemical biosensor, as shown in Scheme 1.

Gel electrophoresis (PAGE) was performed to further characterize the biosensor (Fig. 1B). No new band appeared in the mixture of H0, H1 and H2 in the absence of target miRNA (lane 3), indicating that all hairpin reactants were stable and without false hybridizations. Upon the addition of target miRNA, a new band of high molecular weight appeared (lane 4), which was indicative of the formation of the H1/H2 complex. As expected, CHA was triggered by the T/H0 duplex. Lanes 4–10 show the formation of the DNA TWJ and the capturing capability of the CP strand. When the three hairpins (H0, H1 and H2), L/S and CP were incubated with target miRNA, the bands of H1/H2, L/S and CP attenuated with the appearance of larger molecular weight product band (DNA TWJ) and a new band

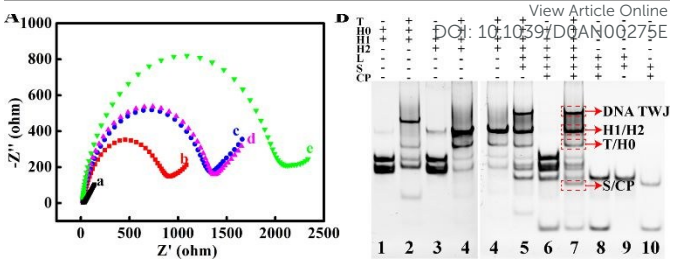

Fig. 1 (A) Characterization of the stepwise modified electrode by EIS: (a) bare AuE, (b) MCH/AuE, (c) CP/MCH/AuE, (d) CP /MCH/AuE incubated with a mixture of H0 (50 nM), H1 (200 nM), H2 (200 nM) and L/S (200 nM), (e) CP/MCH/AuE incubated with a mixture of H0 (50 nM), H1 (200 nM), H2 (200 nM) and L/S (200 nM) and the target miRNA-21(10 nM). (B)PAGE characterization of CHA and the DNA TWJ strategy.

corresponding to the S/CP complex (lane 7). This phenomenon was due to the hybridization of L with the H1/H2 complex to form the stable DNA TWJ complex, and the separation of S from the L/S duplex reacted with CP. No new band was observed in the absence of miRNA-21 (lane 6). (The detail PAGE image was shown in Fig. S1). Taken collectively, these results show that the formation of the DNA TWJ was specific for target-induced assembly, and the CHA-DNA TWJ strategy was highly specific for miRNA detection.

Feasibility of the biosensor

To examine the feasibility of the CHA-DNA TWJ strategy for miRNA detection, miRNA-21, which is always observed to be over-expressed in the tumour tissues, especially in prostate, breast and lung cancers, was selected as the model target. As shown in Fig. 2, when the sensing electrode was incubated with L/S-MB, the intensity of the SWV response was very weak (curve a), indicating that the stability of L/S-MB was higher than that of S-MB/CP. The incubation of a mixture of H1, H2 and L/S-MB with the sensor caused a negligible change in the SWV response (curve b), indicating that DNA TWJ formation was inhibited.

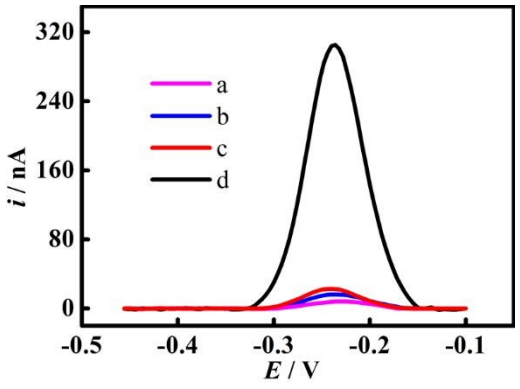

Fig. 2 SWV curves of the CP/MCH/AuE sensor incubated with: (a) L/S-MB (200 nM), (b) a mixture of H1 (200 nM), H2 (200 nM) and L/S-MB (200 nM), a mixture of H0 (50 nM), H1 (200 nM), H2 (200 nM) and L/S-MB (200 nM) in (c) the absence and (d) the presence of miRNA-21 (10 nM).

View Article Online
DOI: 10.1039/D0AN00275E

These findings could be attributed to the ultra-low background reactivity between H1 and H2 in the absence of T/H0. Furthermore, the treatment of the sensor with a mixture of H0, H1, H2 and L/S-MB led to a small SWV response current (curve c), revealing the stability of H0, H1, H2 and L/S in solution. In the presence of miRNA-21 (10 nM), a discernible enhanced current response at about -0.27V was achieved (curve d) corresponding to the electro-oxidation of MB, which indicated that the S-MB strands were brought close to the electrode surface. These results demonstrate the developed CHA-DNA TWJ system could be applied for the detection of target miRNA.

Optimization of the experimental conditions

To achieve excellent performance, the critical experimental parameters, such as the immobilization concentrations of CP and reaction time, were optimized using miRNA-21 as the target. In light of the fact that the surface hybridization was inhibited by the steric hindrance of CP, the effects of different immobilization concentrations of CP were tested. As shown in Fig. 3A, the SWV current signal reached a maximum level at a CP concentration of 0.5 μM and decreased as the concentration escalated from 0.5 to 1.0 μM. Therefore, 0.5 μM was selected as the optimal immobilization concentration of CP for all subsequent experiments. Furthermore, the effect of reaction time was also investigated. Fig. 3B shows that the current signal increased with the prolonged reaction time and approached a plateau after 120 min. There was no obvious change in current after 120 min. Thus, 120 min was employed as the optimal reaction time for all subsequent experiments.

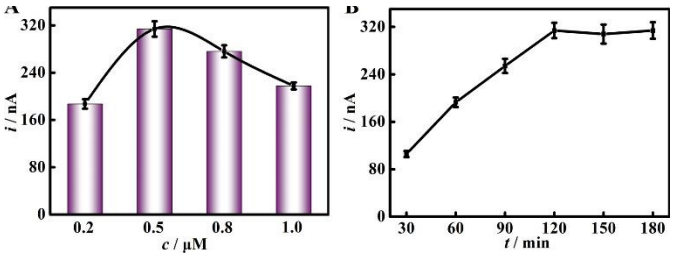

Fig. 3 The influence of CP immobilization concentrations (A) and reaction time (B) on the SWV signal. Error bars: SD; n = 3

Sensitivity of the biosensor

To evaluate the analytical performance of the CHA-DNA TWJ platform, the sensors were investigated by using different concentrations of miRNA-21 based on optimal experimental conditions. Fig. 4A shows that the peak current intensity gradually increased with miRNA-21 concentrations ranging from 0 to 10 nM. Fig. 4B displays that the current intensity was linearly dependent on the logarithmic miRNA-21 concentration ranging from 10 fM to 10 nM. The linear regression equation was i (nA) = 662. 9 + 44.85 lg c (M) (R^2 = 0.9948), and the limit of detection (LOD) was calculated to be 3.6 fM based on the three S/N, which is comparable to the other previously reported approaches listed in Table S2. Furthermore, the reproducibility of this sensing platform was evaluated by a relative standard deviation (RSD) of 4.5%, which revealed satisfactory reproducibility of the sensor.

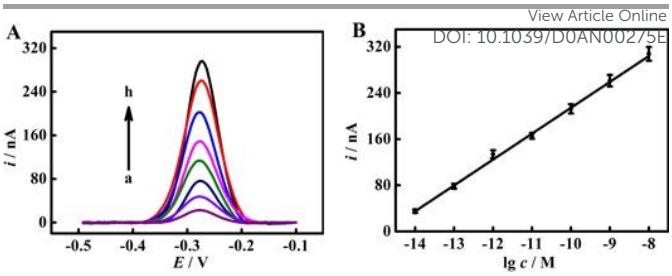

Fig. 4 The sensitivity of the developed approaches. (A) SWV current responses of the present biosensor to different concentrations of miRNA-21(from a to g: 0, 10 fM, 100 fM, 1 pM, 10 pM, 100 pM, 1 nM and 10 nM), (B) Calibration plot of the SWV peak current versus the logarithm of the miRNA-21 concentration. Error bars: SD; n = 3.

To evaluate the generality of the detection strategy, we used the CHA-DNA TWJ system to detect miRNA-141, which is a potentially reliable biomarker of prostate cancer, by changing the specific sequence of H0. A good linearity was also obtained in 7 orders of magnitude from 10 nM to 10 fM. The correlation equation was i (nA) = 679.7 + 46.70 lg c (M) with a correlation coefficient R^2 = 0.9878 (Figure S2A and S2B). And the limit of detection (LOD) was calculated to be 4.5 fM based on the three S/N. These results confirm that our strategy could be easily adapted to different target miRNAs through simply programming the recognition sequences on the H0 to achieve efficient universal detection.

Selectivity of the biosensor

Selectivity is an essential parameter for investigating the specificity of a sensor. Here, we used non-complementary oligonucleotides miRNA-141sequence, single-base-mismatch miRNA-21 (1) and three-base-mismatch miRNA-21 (3) to assess the selectivity for miRNA-21 detection. As shown in Fig. 5, the SWV current response of the miRNA-141 sequence and mismatched sequences were much lower than that of the target

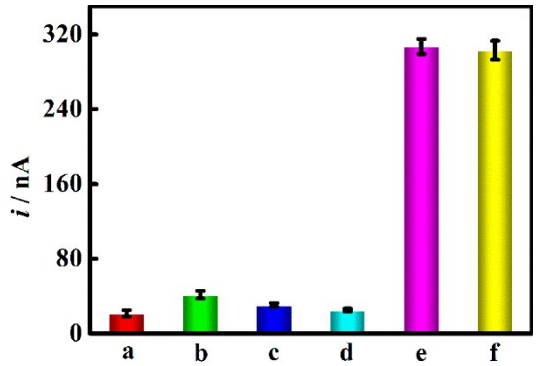

Fig. 5 Selectivity of the biosensor for the target miRNA-21 against different miRNA sequences: (a)blank, (b) single-base mismatched miRNA-21 (1) (100 nM), (c) three-base mismatched miRNA-21 (3) (100 nM), (d) miRNA-141 (100 nM), (e) miRNA-21 (10 nM), and (f) a mixture of single-base mismatched miRNA-21(1) (100 nM), three-base mismatched miRNA-21(3) (100 nM), miRNA-141 (100 nM) and miRNA-21 (10 nM). Error bars: SD; n =3.

View Article Online
DOI: 10.1039/D0AN00275E

miRNA-21. In addition, a mixture of the target miRNA-21 (10 nM) and three other control sequences (each at 100 nM) showed a peak current comparable to that in the presence of miRNA-21 at 10 nM. These results clearly suggest that the fabricated sensor possessed excellent selectivity for miRNA detection and the specificity of the assay was satisfactory.

Detection of miRNA in cancer cells

To explore the feasibility of the developed electrochemical sensor in practical samples, the expression of miRNA-21 was examined in lysates extracted from MCF-7 and Hela cells. As shown in Fig. 6, the peak current response increased slightly as the number of Hela cells increased from 10^1 to 10^5, indicating the low expression of miRNA-21 in the Hela cells. However, the peak current response increased significantly as the number of MCF-7 cells increased from 10^1 to 10^5, implying the high expression of miRNA-21 in the MCF-7 cells. Taken collectively, these results clearly show that the presented biosensing method could detect miRNA-21 in different tumour cells. This method may be a potential tool in real biological samples.

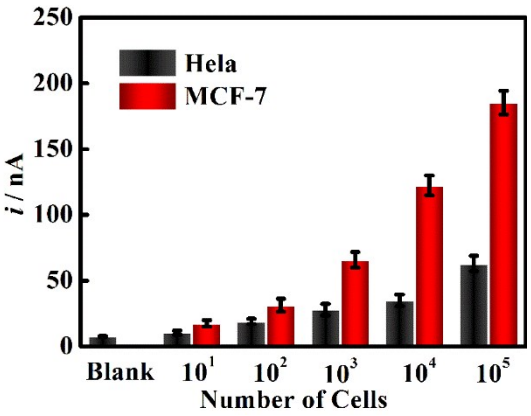

Fig. 6 Determination of miRNA-21 expression in Hela and MCF-7 cells with the developed sensor. Error bars: SD; n= 3.

Conclusions

In conclusion, we have successfully established a universal and enzyme-free biosensor platform that relies on CHA amplification and the DNA TWJ strategy. The presence of miRNA induced the catalytic formation of the H1/H2 duplex via the CHA reaction, which could then hybridize with L/S-MB to form the DNA TWJ. Subsequently, S-MB was released from L/S-MB and hybridized with CP on the sensor electrode, which resulted in a notable current response. Furthermore, the proposed biosensor could be used to detect the miRNA level in lysates derived from tumour cells. The proposed strategy shows features such as simple operation without the participation of any enzymes, high sensitivity, good specificity and universality for target miRNA detection by simply programming the recognition sequences on the hairpin 0. We envision that this proposed biosensor will serve as a potential platform for the early and accurate clinical diagnosis of cancer.

Conflicts of interest

There are no conflicts to declare.

Acknowledgements

This research was supported by the National Key R&D Program of China (No. 2018YFA0902600), National Natural Science Foundation of China (Nos. 21775025, U1705281, U1505221, 21635002), the Program for Changjiang Scholars and Innovative Research Team in University (No. IRT15R11).

Notes and references

1 R. Schickel, B. Boyerinas, S.M. Park, M.E. Peter, *Oncogene*, 2008,**6**,5959-5974.
2 A.M. Cheng, M.W. Byrom, J. Shelton, L.P. Ford, *Nucleic Acids Res.*, 2005,**33**,1290-1297.
3 C. Zhao, G. Sun, S. Li, M.F. Lang, S. Yang, W. Li, Y. Shi, *Proc. Natl. Acad. Sci. U. S. A.*,2010, **107**,1876-1881.
4 H. Zhao, X. Wang, P. Yi, Y. Si, P. Tan, J. He, S. Yu, Y. Ren, Y. Ma, J. Zhang, D. Wang, F. Wang, J. Yu, *Nat. Commun.*, 2017,**8**,1428.
5 B.D. Aguda, Y. Kim, M.G. Piper-Hunter, A. Friedman, C.B. Marsh, *Proc. Natl. Acad. Sci. U. S. A.*, 2008, **105**,19678-19683.
6 S.P. Kabekkodu, V. Shukla, V.K. Varghese, D.S. J, S. Chakrabarty, K. Satyamoorthy, *Rev. Camb. Philos. Soc.*, 2018, **93**,1955-1986.
7 A. Sadlon, P. Takousis, P. Alexopoulos, E. Evangelou, I. Prokopenko, R. Perneczky, *Trends. Mol. Med.*, 2019,**25**,662-672.
8 E.M. Small, E.N. Olson, *Nature,* 2011,**469** ,336-342.
9 W. Yang, J. Ma, W. Zhou, B. Cao, X. Zhou, H. Zhang, Q. Zhao, L. Hong, D. Fan, *Cell Mol. Life Sci.*, 2019,**76**,453-471.
10 Z. Ying, Z. Wu, B. Tu, W. Tan, J. Jiang, *J. Am. Chem. Soc.*, 2017,**139**,9779-9782.
11 Z. Yang, Z. Wen, X. Peng, Y. Chai, W.B. Liang, R. Yuan, *Chem. Commun.,* 2019,**55**,6453-6456.
12 L. Zhong, S. Cai, Y. Huang, L. Yin, Y. Yang, C. Lu, H. Yang, *Anal. Chem.*, 2018, **90**, 12059−12066.
13 J.E. Meis, A. Khanna, *Nature Methods*, 2009,**6**, an12-an13.
14 G.S. Pall, C. Codony-Servat, J. Byrne, L. Ritchie, A. Hamilton, *Nucleic Acids Res.*, 2007,**35**, e60.
15 J. Lee, H. Cho, Y. Jung, *Angew. Chem. Int. Ed.,* 2010,**49**,8662-8665.
16 L. Lu, J. Wang, W. Miao, X. Wang, G. Guo, *Anal. Chem.*, 2019,**91**, 1452-1459.
17 J. Liu, Z. Tang, J. Zhang, Y. Cai, Y. Zhuo, R. Yuan, *Anal. Chem.,* 2018,**90**, 5298-5305.
18 T. Hou, N. Xu, W. Wang, L. Ge, F. Li, *Anal. Chem.*, 2018, **90,** 9591-9597.
19 Y. Wang, L. Xia, C. Wei, H. Wang, H. Wang, R. Yuan, S. Wei, *Chem. Commun.*, 2019, **55**, 13082-13084.
20 X. Wang, T. Hou, H. Lin, W. Lv, H. Li, F. Li, *Biosens. Bioelectron.,* 2019,**137**, 82-87.
21 H. Wang, H. Wang, Q. Wu, M. Liang, X. Liu, F. Wang, *Chem. Sci.,* 2019,**10**,9597-9604.
22 Y. Sun, L. Shi, Q. Wang, L. Mi, T. Li, *Anal. Chem.,* 2019, **91**,3652-3658.
23 B. Bo, T. Zhang, Y. Jiang, H. Cui, P. Miao, *Anal. Chem.,* 2018,**90**, 2395-2400.
24 P. Miao, T. Zhang, J. Xu, Y. Tang, *Anal. Chem.,*2018, **90**, 11154-11160.
25 P. Gai, C. Gu, T., F. Li, *ACS Appl. Mater. Interfaces,* 2018, **10,** 9325-9331.
26 J. Chang, X. Wang, J. Wang, H. Li, Feng Li, *Anal. Chem.,* 2019, **91,** 3604-3610.

View Article Online
DOI: 10.1039/D0AN00275E

27 H. Wang, R. Ma, F. Sun, L. Jia, W. Zhang, L. Shang, Q. Xue, W. Jia, H. Wang, *Biosens. Bioelectron.,* 2018, **122** ,224-230.
28 B. Yang, S. Zhang, X. Fang, J. Kong, *Biosens. Bioelectron.,* 2019, **142**,11544.
29 X. Li, B. Dou, R. Yuan, Y. Xiang, *Sens. Actuators B: Chem.,* 2019,**286**,191-197.
30 C. Xing, J. Dai, Y. Huang, Y. Lin, K.L. Zhang, C. Lu, H. Yang, Small, 2019,**15**, e1901795.
31 H. Cheng, W. Li, S. Duan, J. Peng, J. Liu, W. Ma, H. Wang, X. He, K. Wang, *Anal. Chem.,* 2019,**91**, 10672−10678.
32 H. Wang, C. Li, X. Liu, X. Zhou, F. Wang, *Chem. Sci.*, 2018,**9** ,5842-5849.
33 Y.S. Jiang, B. Li, J.N. Milligan, S. Bhadra, A.D. Ellington, *J. Am. Chem. Soc.,* 2013,**135**,7430-7433.
34 P. Yin, H.M. Choi, C.R. Calvert, N.A. Pierce, *Nature,* 2008,**451** ,318-322.
35 D.R. Boer, J.M. Kerckhoffs, Y. Parajo, M. Pascu, I. Uson, *Angew. Chem. Int. Ed.,* 2010,**49**,2336-2339.
36 S. Hamada, S. Murata, *Angew.Chem. Int. Ed.,* 2009, **48**, 6820-6823.
37 D. Shu, Y. Shu, F. Haque, S. Abdelmawla, P. Guo, *Nat Nanotechnol*,2011, **6**, 658-667.

View Article Online
DOI: 10.1039/D0AN00275E

For Table of Contents Only

A catalyzed hairpin assembly and binding-induced formation of DNA three-way junction for ultrasensitive electrochemical detection of diverse miRNAs is reported.